

# **Analysis of soot emissions through the development of phenomenological soot model using gasoline-ethanol blend for gasoline compression ignition combustion: A CFD Simulation Study**

Prakash Koirala

## **Abstract**

In the current study, computational fluid dynamics (CFD) simulation was performed of a single-cylinder gasoline compression ignition (GCI) engine of gasoline-ethanol blend ratios of E10 and E50. The engine CFD model was validated against experimental data collected at -25 CAD SOI1 timing. The model was validated for RD5-87 which showed similar characteristics of E10 with 87% iso-octane and 13% nheptane by mass fraction. The trend of soot emissions increment was observed with a change in SOI1 timings which showed  $\text{SOI } -31 > \text{SOI } -25 > \text{SOI } -19 \text{ CAD aTDC}$ . The effect of SOI1 timing and fuel composition were studied which showed E50 has lower soot emissions compared to E10 which was due to higher oxygen content on ethanol causing the soot to get oxidized. Soot oxidation was found to be higher for -19 CAD due to higher OH radical formation within the cylinder. Soot number density was also measured and found to be higher for the E10 case as compared to E50 for SOI timing of -31 CAD.

## **Modeling Methodology:**

### ***CFD Model Computational Framework***

A 3D CFD model was created using CONVERGE CFD software. Different parts such as cylinder head, liner, piston, intake and exhaust ports, valve stems, valve seats and valve faces were imported using STL format. A RNG k- $\epsilon$  model is used for turbulence modeling. Similarly, the atomization and breakup of fuel droplets is modeled via the Kelvin-Helmholtz and Rayleigh-Taylor (KH-RT) hybrid model. This model considers the instabilities of both Kelvin-Helmholtz and Rayleigh-Taylor due to the combination of which a realistic atomization and breakup could be predicted. Figure 1 shows the computational model developed for the single-cylinder GCI engine. A 3mm base grid was prescribed throughout the entire geometry and then the grid was refined to 0.75mm inside the combustion chamber, 0.3mm around the intake and exhaust valves in the area where the incoming or outgoing fluid flows when the valves were open, 0.18mm around the injector during the injection event and 1 mm near the piston crown to resolve near-wall conditions better using the fixed embedding method.

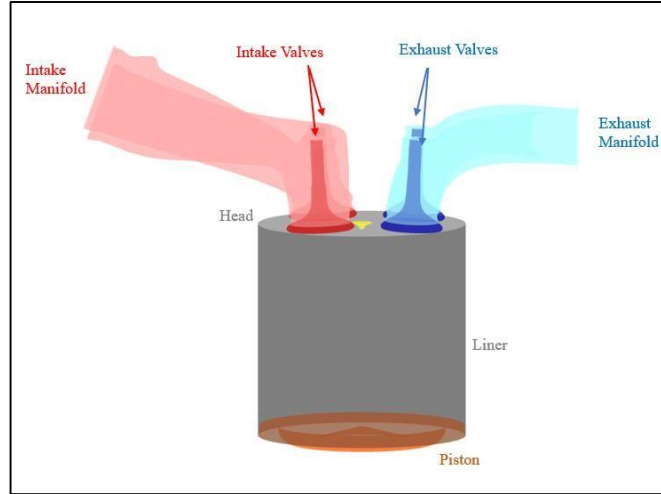


*Figure 1 Computational model developed for GCI Engine*

The dynamic drop drag model of Liu et al. was used for the calculation of the droplet drag coefficient. This model calculates the drop drag coefficient dynamically as the flow condition changes to determine a more accurate drag coefficient. Similarly, for drop evaporation, the Frossling correlation was used which is needed to convert liquid into gaseous vapor and to determine the time rate of change of droplet size. Finally, a spray sub-model was also used to describe the interaction between the fuel spray and the engine walls. Table 1 lists the specifications of this engine.

*Table 1 Specifications of single-cylinder GCI engine*

Bore	82mm
Stroke	80.1mm
Connecting Rod Length	152.4mm
Geometric Compression Ratio	15.6:1
Intake Opening/ Closing	-360/-150 CAD aTDC
Exhaust Opening/ Closing	127/358 CAD aTDC
Engine speed (rpm)	1500

The specifications of the GDI injector and its specifications is provided in Table 2.

*Table 2 Injector Specifications*

No. of nozzle holes	8
Nozzle diameter [ $\mu\text{m}$ ]	110
Spray included Angle [ $^\circ$ ]	150
Spray Cone Angle [ $^\circ$ ]	17
Nozzle Discharge Coefficient [-]	0.79
Experimental operating pressure [bar]	10
Injection duration	5.9 CAD

SOI	-25 CAD, 0 CAD
Injection pressure	700 bar

SAGE detailed chemistry solver was used to simulate the in-cylinder heat release developed by Seneca et al. Presently, RD5-87 gasoline containing 10% (by volume) ethanol that has an anti-knocking index of 87 was used as the baseline fuel [4]. So, PRF blend of 87% iso-octane and 13% n-heptane by mass fraction replicated the behavior of RD5-87 at these conditions for E10 fuel. Similarly, the chemical properties of E50 fuel were referred and used to simulate the model.

## Results and Discussions

Dalian phenomenological soot model was used that involves soot precursor formation, nucleation and growth, coagulation and oxidation, soot particle size distribution and emission prediction. The initialized factors for this soot model is given in Table 3 below. These factors were initialized in response to the literature study done for GCI combustion.

*Table 3 Initialized factors for soot modeling*

Soot inception pre-exponential factor	1e+11
Soot coagulation factor	2.0
Soot oxidation of OH collision factor	0.13
Soot surface growth factor	10500

### **Model Validations**

The CFD model was validated for E10 fuel for four SOI timings. The experimental data was collected at 25 CAD aTDC. The experimental pressure trace is an average of 300 consecutive cycle, whereas the simulated pressure traces is taken from the result of third CFD cycle. The CFD model captures the average cylinder pressure and AGHRR reasonably well for all SOI timings. However, the gross heat release rate is slightly overpredicted by the model. This level of uncertainty is probably due to the differences between chemical kinetics mechanism and actual kinetics. It should be noted that in CFD modeling the heat release rates are usually harder to match with experimental results due to the sensitivity

of heat release rate to temperature distribution and chemical kinetics mechanism.

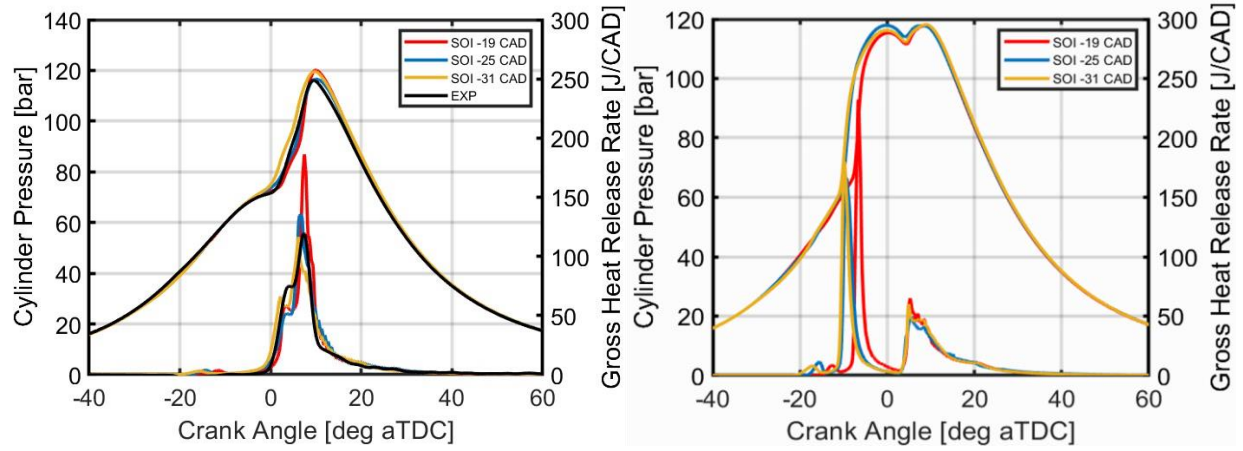


Figure 2 Model Validation for E10(left) and E50 (right) case. CFD model was only ran for the E50 case

The time between the start of injection (SOI1) and the start of combustion is referred as ignition delay time. The ignition delay time for different SOI timings were calculated and were -19/-25/-31 CAD aTDC were 21.9/27.3/40.8 respectively. The ignition delay time was found to increase with SOI timing. This is since the in-cylinder region is cooled at initial conditions and injecting more fuel will lead to increase in the ignition delay time.

Table 4 Combustion Phasing for different SOI1 conditions for E10 fuel

SOI1 [CAD aTDC]	-19	-25	-31
CA0	-17	-21.5	-26.8
CA10	1.2	1.3	3.8
CA50	7.6	7.4	8.7
CA90	19.1	18.4	19.2

The ignition delay time was found to decrease with advancement in SOI1 but the combustion duration was found to decrease. The combustion duration decreases by about 1.7 CAD when SOI is advanced from -25 CAD to -31 CAD. This reduction is due to greater thermal and mixture stratification enabling autoignition to happen in a more step-by-step manner.

Table 5 Ignition Delay and Combustion Duration for E10 fuel

SOI1 [CAD aTDC]	IDT [CAD]	Combustion Duration [CAD]
-19	21.9	17.9
-25	27.3	17.1
-31	40.8	15.4

Figure 3 shows the plot of the ratio of fuel film mass on the piston to the total fuel mass injected for all SOI conditions. The ratio was increased with advancement in SOI1 for all the cases. Here, the evaporation time for the fuel film was significantly higher and is not readily available for combustion.

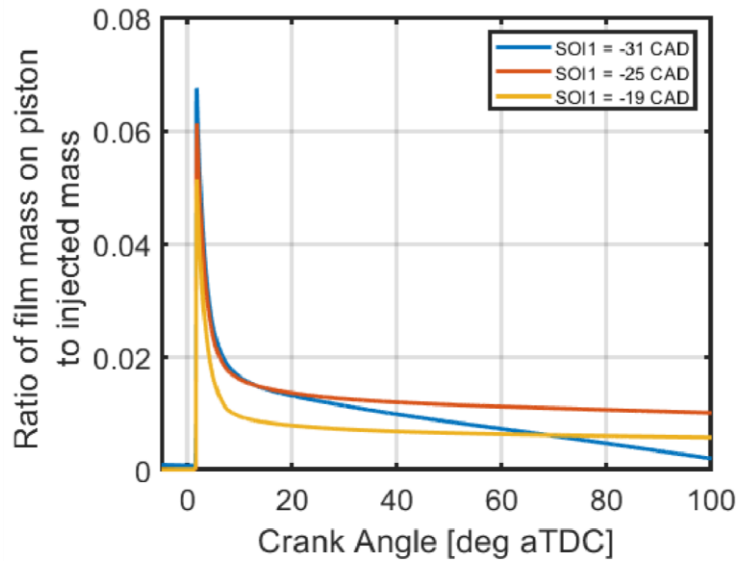


Figure 3 Ratio of fuel mass on piston to the total injected mass

The total soot mass was found to be maximum for -31 SOI1 injection timing. The soot mass found to decrease in the order of SOI -31 > SOI -25 > SOI -19. Figure 4 presents the soot emissions from E10 fuel for all SOI conditions. As we know, soot is formed in rich regions, in a temperature range of about 2000K which is due to the deposition of fuel films near wall regions. The higher temperature within the incylinder conditions causes fuel films to evaporate and produces more soot. In the current study, there was a significant amount of fuel film formed on the piston walls due to the impingement. It was also seen that the film mass increases with advancement in SOI1. Figure 5 shows the cut-plane visualizations for E10 and E50 fuel that shows soot mass impinging on the piston bowl (E10 > E50)

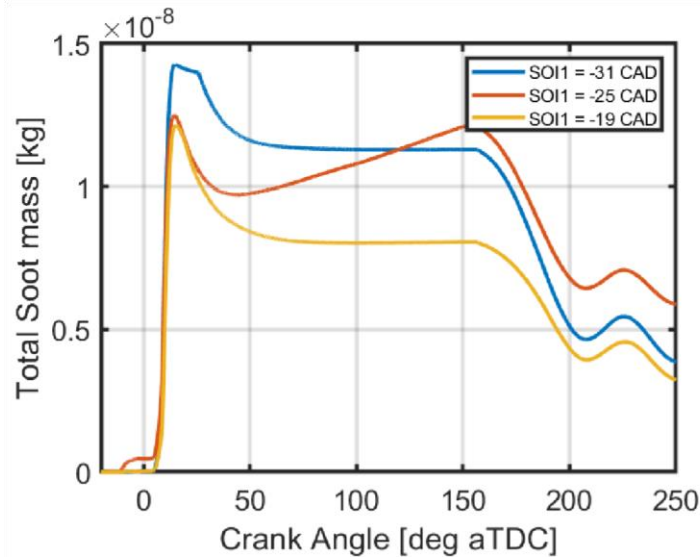


Figure 4 Total Soot mass formed for E10 fuel.

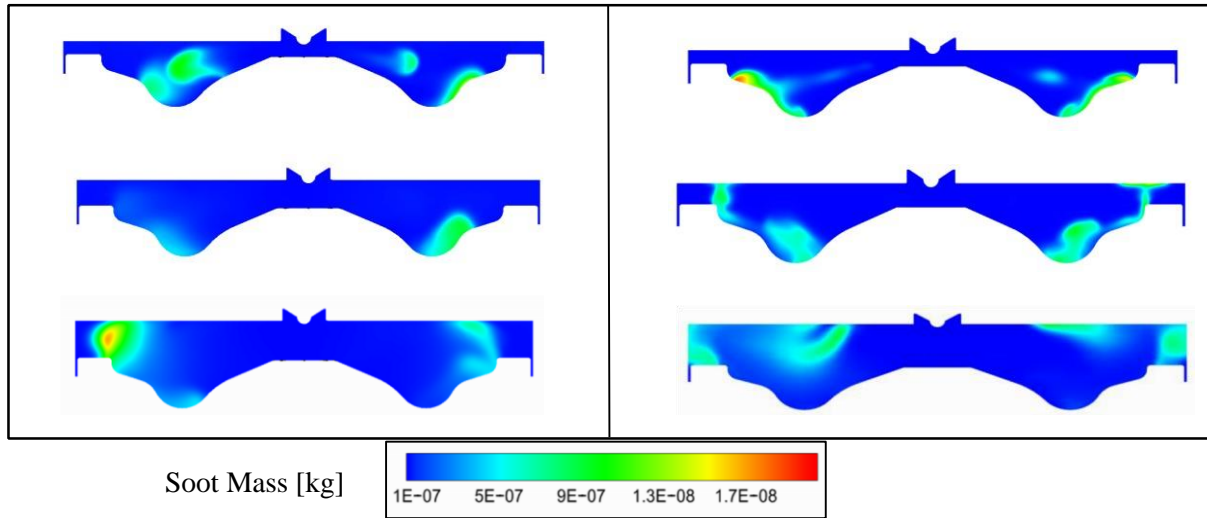


Figure 5 Cut-plane visualizations for total soot mass in (kg) for E10 (left) and E50 (right) for different crank angles 10(third), 20(second) 30 CAD (first) aTDC.

Like the case of E10, the total soot mass for E50 was found to be maximum for -31 SOI1 timing. The total soot mass is in the order of SOI -31 > SOI -25 > SOI -19 CAD. Figure 6 presents the soot emissions from E50 fuel for all SOI conditions. The total soot mass was comparatively low which is due to the higher oxygen content which promotes more complete combustion, resulting in fewer partially burned soot particles during the combustion process as compared to E10. The amount of peak soot mass was reduced by amount of  $0.4\mu\text{g}$  as compared to both the cases.

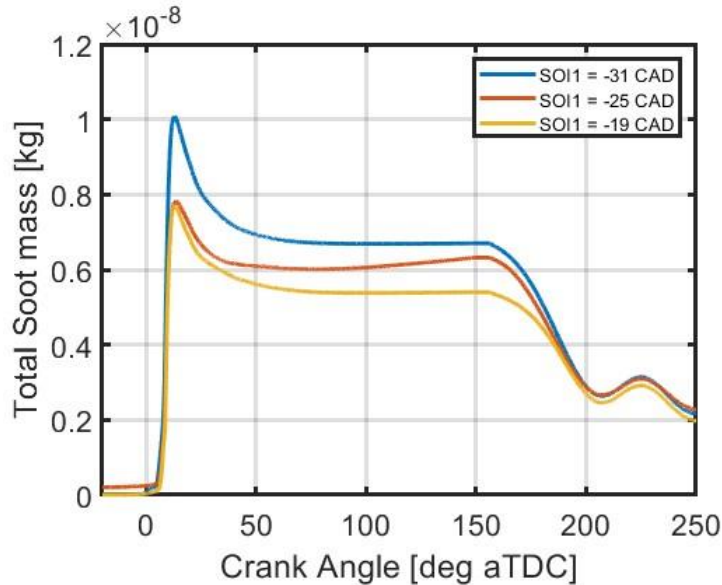


Figure 6 Total Soot mass formed for E50 fuel.

As SOI timing is advanced, it allows more time for mixing, and produces higher amount of soot for -31 CAD. This is due to the accumulation of fuel film on the walls of cylinder because of lower temperature inside the cylinder. Due to such lower temperature inside cylinder, the evaporation of liquid fuel is less that ultimately causes higher fuel film formation on the walls. Further, it is noticed that for SOI1 timing of -31 CAD, more fuel mass was near the piston bowl as compared to -25 CAD. Also, the soot oxidation process

was higher due to the more amount of OH radical formed inside the cylinder. The higher amount of OH radical was formed in the cylinder at -19 CAD aTDC that causes more amount of soot to get oxidized within the cylinder causing lower amount of soot emissions.

Injecting fuel earlier in the cycle tends to increase the concentration of soot while delaying the injection timing reduces the concentration. The highest concentration of soot particles was observed at SOI timing of -31 CAD whereas the lowest was observed at SOI timing of -19 CAD.

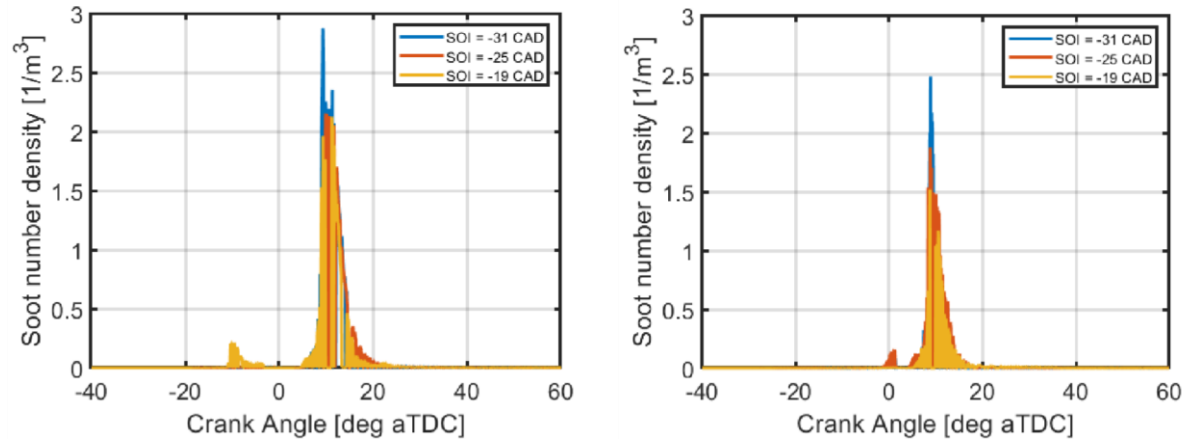


Figure 7 Soot number density for E10 (left) and E50 (right) fuel.

A higher fuel film was accumulated due to restriction in evaporation process due to cooler conditions. E10 was found to have a significant impact on combustion duration due to the higher fuel film. The heat of vaporization and viscosity of E50 is greater than E20 but both has almost similar densities. So due to higher heat of vaporization more fuel mass impinges and due to lower in cylinder temperature respective fuel film is formed with respect to E10 and E50. Further, due to the higher heat of vaporization and viscosity E50 fuel was found to have higher fuel films than E10.

## Conclusions

This study shows the effect of start of injection timing, and fuel composition on the soot emissions for gasoline ethanol blend ratios of E10 and E50 under ten bar conditions. The CFD model was first validated with the experimental data collected under light duty GCI engine under same operating conditions at -25 SOI1 timing. The soot emissions was found to be maximum for -31 CAD SOI1 conditions and followed the trend SOI -31 > SOI -25 > SOI -19 CAD. The amount of soot mass was found to be lower for E50 comparatively. It was identified that the due to higher ethanol content renders to produce less soot for E50 case. For the SOI timing of -31 CAD aTDC, higher amount of soot was seen which was due to higher film mass accumulation on the piston walls as compared to -25 CAD and -19 CAD. In summary, the effects of fuel composition and start of injection timing (by varying start of injection (SOI1) timing) was studied on combustion duration and soot emissions for gasoline ethanol blend of E10 and E50. **References**